Maejo Int. J. Sci. Technol. **2022**, *16*(03), 275-290

Maejo International Journal of Science and Technology

ISSN 1905-7873
Available online at www.mijst.mju.ac.th

Full Paper

A novel iterative finite element optimisation method of solving inverse problem of electrocardiography to localise ischemic region on the heart

Hamed Kaghazchi [1,*] and Mustafa Kerem Ün [2]

[1] Faculty of Engineering, Baku Engineering University, Baku, Azerbaijan
[2] Faculty of Engineering, Cukurova University, Adana, Turkey
* Corresponding author, e-mail: hkaghazchi@beu.edu.az

Received: 13 June 2022 / Accepted: 25 December 2022 / Published: 27 December 2022

Abstract: The inverse problem of electrocardiography (ECG) involves determining the transmembrane potential distribution within the heart from the ECG readings taken from the torso. The problem bears importance since its solution prescribes a tool for identifying various heart anomalies including locating the ischemic zone in the heart. The solution of the inverse problem is typically achieved by running a finite element simulation and obtaining a matrix relationship between torso potentials and the transmembrane potentials. The resulting system is usually underdetermined and solved with constraint optimisation (i.e. regularisation), where various constraints have been utilised in the literature.

In this work we introduce a novel, regularisation-free iterative technique that uses finite element optimisation to tackle the inverse problem and locate the ischemic zone in the heart. The technique relies on a simple parametrisation of the location of the ischemic region in a bidomain heart model and eliminates the need for regularisation applied in the existing methods. The parameters are iteratively evolved using a sensitivity analysis and, when converged, indicate the location of the ischemic zone. The method is observed to successfully find the ischemic region, independent from where it is located in the heart.

Keywords: electrocardiography, finite element optimisation, ischemic region, inverse problem

INTRODUCTION

Many heart problems are closely linked with disturbances in the heart's electrical conduction system. The standard method to identify those anomalies in a clinical setting is electrocardiography (ECG). Due to the public health impact of those anomalies, the conduction in the heart has also been a subject of mathematical simulation studies. Reconstructing the torso potentials from a given

Maejo Int. J. Sci. Technol. **2022**, *16*(03), 275-290

dipole source in the heart (or equivalently a given transmembrane potential distribution) is called *the forward problem* of ECG. The counterpart of the forward problem is the more challenging *inverse problem* of ECG, which involves determining the transmembrane potential distribution within the heart from the ECG readings taken from the torso.

The inverse problem of ECG has been a research area since 1980s [1]. It is more reminiscent of the actual diagnostic process and clinicians 'solve' this problem every day by observing the torso ECG readings in order to make deductions about the patient's heart. Yet, ECG is not always effective for the identification of certain conditions such as ischemia, which makes the mathematical analysis of the inverse problem an important research topic [2-4].

Ischemia is a relatively common heart condition caused by insufficient oxygen supply to the heart muscle due to reduced blood flow to the tissue. During the ST segment of ECG, the whole heart muscle is in a depolarised stage where the transmembrane potential (TMP) has a plateau value of 0 mV for healthy tissue. On the other hand, TMP has an abnormal value of -30 mV in the ischemic tissue. Hence the clinical sign for acute myocardial ischemia is a shift of the ST segment of ECG relative to the healthy level, whose magnitude depends on the size and location of ischemic region in the heart tissue (as well as the location of recording electrodes on the patient's torso). However, despite many years of research and clinical practice, ECG has a modest sensitivity and specificity (65-80%) in detecting and especially in localising myocardial ischemia [5, 6].

Ischemia has been a main focus of the numerical studies to tackle both forward and inverse problems of ECG. The *finite element method* (FEM) is widely utilised in these studies [7, 8]. Numerical detection of the ischemic zone in the heart relies on the shifted TMP during the ST segment. When the TMP distribution in the heart can be reconstructed from the measured torso potentials through FEM, the location of nodes with shifted potentials indicate the ischemic zone.

The solution of the inverse problem is mathematically more challenging since it is ill-conditioned and requires some sort of optimisation to find the 'best solution' among the pool of candidate solutions [9]. This is typically achieved by running an FEM simulation and obtaining a matrix relationship between the torso potentials and the TMPs as

$$\mathbf{K}\boldsymbol{\Phi}_H = \boldsymbol{\Phi}_T \tag{1}$$

where $\boldsymbol{\Phi}_H$ is the vector of unknown nodal TMPs within the heart region, $\boldsymbol{\Phi}_T$ is the vector of the given nodal torso potentials and $\mathbf{K}$ is a stiffness matrix obtained from the FEM formulation. Since the above system is underdetermined and highly ill-conditioned, a solution can be found only through *regularisation*, which is the mathematical technique of constraining an ill-posed problem so as to convert it to a better-posed one.

Regularisation is a principal topic in inverse problem research, and there is vast literature on regularisation [10-15]. Since the above system is underdetermined and highly ill-conditioned, a solution can be found only by minimising the error norm $\left\|\mathbf{K}\boldsymbol{\Phi}_H - \boldsymbol{\Phi}_T\right\|$ under some regularisation of the solution as

$$\min\left\{\left\|\mathbf{K}\boldsymbol{\Phi}_H - \boldsymbol{\Phi}_T\right\| + \alpha\left\|\mathbf{L}\boldsymbol{\Phi}_H\right\|\right\} \tag{2}$$

where $\mathbf{L}$ is a regularisation matrix and α is the regularisation parameter. Here, different choices for $\mathbf{L}$ may change the effectiveness of the approach significantly and the optimal value of α is usually found by trial and error, which is computationally inconvenient and is the main drawback of this approach.

Maejo Int. J. Sci. Technol. **2022**, *16*(03), 275-290

Despite these drawbacks, the regularisation-based solution of the inverse problem has always been common practice and used extensively in the literature. Messinger-Rapport and Rudy [16, 17] compared several variations of Tikhonov regularisation (zero-, first- and second-order) and found that zero-order Tikhonov regularisation performed as well as those of higher order. Spatially adaptive FEM schemes with local regularisation have been tried [18]. In another approach [19] optimisation was done over the time integral of TMP over the ST segment rather than at one time instant, making the inverse solution more robust to input noise but limiting its applicability to identifying activation. Novel spatiotemporal regularisation approaches suitable for recovering the TMP at the heart surface [20] and characterising myocardial infarctions [21] through inverse ECG modelling have been proposed. The Tikhonov regularisation method, where regularisation parameter is obtained with composite residual and smoothing operator, was also used to stabilise the inverse procedure [22].

There are several more recent studies done on the inverse problem of ECG, proving the actuality of the topic despite its early origin. These studies discussed several related issues such as the impact of the utilised torso model on the solution [23], further evaluation and improvements in regularisation methods [24, 25], and potential use of artificial intelligence techniques in inverse modelling [26, 27]. In the present work an entirely new, regularisation-free numerical approach is proposed to solve the inverse problem of ECG. The method is based on a simple parametrisation of the ischemic region, something that has not been done in the existing literature. In the proposed method the ischemic region of the heart is located iteratively through finite element optimisation in a novel manner. The optimisation scheme updates the parameters through a sensitivity analysis to reconstruct the TMPs in order to localise the ischemic region.

METHODS

The sensitivity-based iterative optimisation approach proposed here is an entirely new approach to tackling the inverse problem of ECG. We describe in this section the related finite element formulation and sensitivity procedure. The bidomain model of the heart is described in detail first. Next, the general sensitivity analysis is explained with respect to how it is used as an iterative optimisation tool in this problem. The computer implementation of the FEM and the sensitivity-based optimisation is also briefly mentioned in this section.

Bidomain Model of Heart Conduction

As myocardial ischemia can be characterised by the altered TMP of the tissue, reconstructing a whole-heart TMP map will promote the determination of the location and extent of ischemia [5, 28, 29]. The inverse problem of ECG is usually formulated based on the bidomain heart model, where extracellular and intracellular environments are taken as overlapping continua. The cardiac source is represented either by the myocardial TMP or the current density derived from it [29, 30]. Since capacitive and inductive effects are negligible in the heart [9], torso potentials at a time instant depend only on the TMP distribution at the same time instant. During the ST interval, the TMP has a homogeneous plateau value of 0 mV throughout the healthy heart tissue. Its value drops to -30 mV in the ischemic region of the heart [31-34]. Consequently, the inverse problem for the purpose of locating the ischemic tissue is typically formulated in the ST interval of the heart cycle, where healthy and unhealthy tissue can be distinguished merely from their TMP values.

Let V_m denote the TMP during the ST interval; then

Maejo Int. J. Sci. Technol. **2022**, *16*(03), 275-290

$$V_m(x) = \begin{cases} 0\text{ mV}, & \text{x in healthy tissue} \\ \text{-30 mV}, & \text{x in ischemic tissue} \end{cases} . \tag{3}$$

The quasi-static bidomain model and its clinical meaning is summarised in this section. The problem domain, which consists of the heart (designated as *H*) and the torso (designated as *T*), satisfies a Poisson partial differential equation as

$$-\nabla \cdot (\boldsymbol{\sigma}(x)\nabla\Phi(x)) = f(x), \qquad x \in \Omega \tag{4}$$

where Φ is the potential and *f(x)* is given as

$$f(x) = \begin{cases} 0, & x \in T \\ \nabla \cdot \boldsymbol{\sigma}_i \nabla V_m(x), & x \in H \end{cases} . \tag{5}$$

Here, $\boldsymbol{\sigma}$ is the conductivity tensor expressed as

$$\boldsymbol{\sigma}(x) = \begin{cases} \sigma_T \mathbf{I}, & x \in T \\ \boldsymbol{\sigma}_i + \boldsymbol{\sigma}_e, & x \in H \end{cases} .$$

The *f(x)* term for the heart (*H*) represents the source with the differing V_m in the ischemic tissue. It should be noted that if the heart is entirely healthy, ∇V_m will vanish in the entire heart domain and there will be no source. In this case the problem has a trivial (i.e. zero) solution for Φ, which is observed in the ST segment of the ECG of a healthy heart. Φ represents the electrostatic potential within the torso and Φ_e is the extracellular potential within the heart :

$$\Phi(x) = \begin{cases} \Phi & x \in T \\ \Phi_e & x \in H \end{cases} . \tag{6}$$

The conductivities of intracellular and extracellular mediums of the heart are $\boldsymbol{\sigma}_i$ and $\boldsymbol{\sigma}_e$ respectively. The conductivities of various tissues in the torso region are represented by σ_T. Since these conductivities are isotropic, the conductivity tensor is a multiple of identity tensor **I**.

On the other hand, the heart has anisotropic conductivity with differing conductivity values perpendicular to σ_l and along the heart muscle fibres σ_t. Thus, the conductivity tensor of the heart expressed in muscle fibre coordinates can be written as

$$\boldsymbol{\sigma}_h^* = \begin{bmatrix} \sigma_l & 0 \\ 0 & \sigma_t \end{bmatrix} \qquad \text{h=}i \text{ or } e \quad , \tag{7}$$

where the index h refers to either intracellular (*i*) or extracellular (*e*) medium. In finite element (FE) formulation this tensor is transformed to the Cartesian coordinates at each element as

$$\boldsymbol{\sigma}_h = \mathbf{A}\boldsymbol{\sigma}_h^* \mathbf{A}^T \tag{8}$$

where **A** is an orthogonal rotation matrix given by

$$\mathbf{A} = \begin{bmatrix} \cos\theta & \sin\theta \\ -\sin\theta & \cos\theta \end{bmatrix} . \tag{9}$$

Here, the angle θ represents the rotation of the heart fibre with respect to Cartesian axes. In the literature the following formula for the angle θ is proposed for a two-dimensional heart model:

$$\theta(x, y) = \tan^{-1}\left(\frac{K_T x + K_N y}{1 + K_N x - K_T y}\right) , \tag{10}$$

Maejo Int. J. Sci. Technol. **2022**, *16*(03), 275-290

which we have utilised in this work. The related constants are $K_T = 0.3$ and $K_N = 0.2$.

Boundary conditions require that no current flows out of the torso and are expressed as

$$(\sigma_T \nabla \Phi) \cdot \mathbf{n}_T = 0 \qquad on\ \partial T \ . \tag{11}$$

The heart and torso potentials match at the heart-torso boundary and are expressed as

$$\Phi_e = \Phi \qquad on\ \partial H \quad , \tag{12}$$

and the current flowing across the heart boundary should be continuous and is expressed as

$$(\boldsymbol{\sigma}_e \nabla \Phi_e) \cdot \mathbf{n}_H = -(\sigma_T \nabla \Phi) \cdot \mathbf{n}_T \quad on\ \partial H \ . \tag{13}$$

In the above equations ∂ signifies the boundary of the corresponding domain.

Finite Element Optimisation Based on Sensitivity Analysis

The FE weak form of the problem is obtained after applying the Galerkin method and Green's theorem to Eq.2 and imposing the natural boundary conditions to the resulting expression:

$$\int_{\Omega} (\sigma(x) \nabla \Phi(x)).\nabla w(x) dx = -\int_{H} (\sigma_i \nabla V_m(x)).\nabla w(x) dx \ , \tag{14}$$

where $\Omega = T \cup H$ represents the entire problem domain [5, 31, 35-38].

Using standard linear functions for shape and weighting functions, the weak form eventually leads to a linear system as

$$\mathbf{K}_g \boldsymbol{\Phi} = \mathbf{f} \ . \tag{15}$$

Here, $\mathbf{K}_g$ represents the global stiffness matrix. The force vector **f** of this system is formed by the source term. In the case of healthy tissue, **f=0** and the system has a trivial (i.e. zero) solution corresponding to a healthy ST segment. In the presence of ischemic tissue, **f** takes a non-zero value giving a non-zero solution for Φ, which is associated with the ST-segment shift.

In many engineering optimisation problems the quantity to be optimised has (or is assumed to have) a functional form, and optimisation is achieved by optimising the parameters of this function. The simplest example of this approach is the statistical regression. In FEM, input parameters can be optimised, which will produce a specific output. The relation between the FE input data (geometry, material properties, boundary conditions, etc.) and the FE output (nodal solutions) is mathematically more complex, yet this approach is frequently applied in material property estimation or topology optimization [39, 40]. To apply the FE optimisation to the inverse problem of ECG (i.e. the localisation of the ischemic region), we parameterise the TMP distribution and optimise the location of the ischemic region with respect to these parameters.

For clarity, we illustrate the method on a realistic 2-D torso geometry. We have assumed a continuous functional form for TMP given by

$$V_m = A[-\arctan(B(x-a)) + \arctan(B(x-b))] \cdot [-\arctan(B(y-c)) + \arctan(B(y-d))] \ . \tag{16}$$

The defined function takes a value of 0 mV everywhere except a rectangular-like region where it smoothly decreases to -30 mV (Figure. 1). This region signifies the ischemic region in the heart, and its size and location depend continuously on the parameters *a*, *b*, *c* and *d* of the function. The functional form prescribed by Eq.16 prevents the TMP from fluctuating from one node to the other and 'regularises' the TMP distribution and hence the shape of the ischemic region. It is also an advantage that the location of the ischemic region in the heart is described using only four

Maejo Int. J. Sci. Technol. **2022**, *16*(03), 275-290

parameters. The factor A is adjusted such that the minimum value of the function is equal to -30. (The value of A changes with the values of a, b, c and d.) The multiplier B is chosen to adjust the width of the transition zone, designated as H, where TMP changes from a value of 0 mV to -30 mV. For the physiologically realistic value of H=1 mm, B is approximately equal to 5. Parametrisation of V_m per Eq.12 gives V_m a smooth functional form and prevents it from fluctuating. In other words, enforcing V_m to take a certain functional form regularises this quantity, which is necessary in tackling inverse problems.

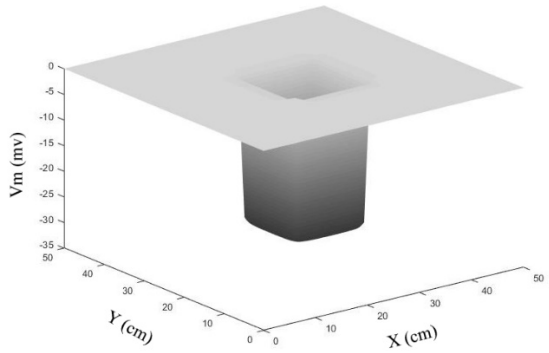

Figure1. TMP function

Assume that there exists an ischemic region in the heart, whose TMP is represented with Eq.16. Let **e** denote the vector of a set of non-zero torso potentials caused by the presence of the ischemic region. The values in **e** can be either observed experimentally or equivalently calculated in a numerical experiment simulating the forward problem with imposed ischemia. Let **y** indicate the vector of the same torso potentials estimated by the FE simulation, whose values depend on the parameters a, b, c and d used in the FE run:

$$\mathbf{y} = \mathbf{y}(a,b,c,d) \quad . \tag{17}$$

The *objective function* J is a measure of the difference between the experimentally measured **e** and estimated torso potentials **y**:

$$J = J(\mathbf{e}, \mathbf{y}(a,b,c,d)) \quad . \tag{18}$$

Let **p** be the column vector that contains the parameters a, b, c and d:

$$\mathbf{p} = \begin{bmatrix} a \\ b \\ c \\ d \end{bmatrix} \quad . \tag{19}$$

The simplest possible J would sum the square errors for each torso potential and can be expressed in matrix form as

$$J = \|\mathbf{e} - \mathbf{y}(\mathbf{p})\| = (\mathbf{e} - \mathbf{y}(\mathbf{p}))^T (\mathbf{e} - \mathbf{y}(\mathbf{p})) \quad . \tag{20}$$

In general, the relation between **y** and a, b, c and d is non-linear, independent from the linearity of the problem. Hence the objective function is also highly non-linear. Yet, since the objective function depends continuously on parameters in **p**, an iterative gradient method can be devised for

Maejo Int. J. Sci. Technol. **2022**, *16*(03), 275-290

the minimisation of the objective function. In other words, an extra regularisation term as in Eq.2 is not necessary since the solution is already regularised by adopting a functional form for V_m.

Objective Function Minimisation

To derive the iteration scheme, we have taken the variation of the objective function with respect to an infinitesimal change in the parameter vector **p** and set it to zero, an obvious way to find the extremum of a function. The variation of Eq.20 with respect to the variation in **y** can be expressed as

$$\delta J = (\delta \mathbf{y}(\mathbf{p}))^T (\mathbf{e} - \mathbf{y}) + (\mathbf{e} - \mathbf{y})^T (\delta \mathbf{y}(\mathbf{p})) = 0 \quad . \tag{21}$$

Using the variation in the parameter **p**, the vector $\delta\mathbf{y}$ can be written as

$$\delta \mathbf{y}(\mathbf{p}) = \frac{\partial \boldsymbol{y}(\mathbf{p})}{\partial \mathbf{p}} \partial \mathbf{p} = \mathbf{S} \delta \mathbf{p} \quad , \tag{22}$$

where

$$\mathbf{S} = \frac{\partial \boldsymbol{y}(\mathbf{p})}{\partial \mathbf{p}}$$

is called the *sensitivity matrix* and describes the change in the FE simulation output **y** with respect to a change in **p**. Substituting (18) into (17) gives

$$\delta J = (\mathbf{S}\delta \mathbf{p})^T (\mathbf{e} - \mathbf{y}(\mathbf{p})) + (\mathbf{e} - \mathbf{y}(\mathbf{p}))^T (\mathbf{S}\delta \mathbf{p}) = 0 \tag{23}$$

Since *J* is a scalar, both terms of the above matrix expression are equal to each other, which allows Eq. 23 to be written as

$$\delta J = \delta \mathbf{p}^T \mathbf{S}^T (\mathbf{e} - \mathbf{y}(\mathbf{p})) = 0 \quad . \tag{24}$$

Since $\delta\mathbf{p}$ is arbitrary, the above equation holds only if

$$\mathbf{r}(\mathbf{p}) = \mathbf{S}^T (\mathbf{e} - \mathbf{y}(\mathbf{p})) = \mathbf{0} \quad . \tag{25}$$

Here $\mathbf{r}(\mathbf{p})$ is the residual which approaches **0** as the predicted potential **y** approaches the actual potential **e**. Eq.25 represents a non-linear system of equations in **p**, whose solution minimises the objective function *J*. The system is solved through Newton-Raphson iteration. If $\mathbf{p}_k$ is the estimate of **p** obtained at the *k*th iteration, the system is linearised at $\mathbf{p}=\mathbf{p}_k$ as

$$\left. \frac{\partial \mathbf{r}}{\partial \mathbf{p}} \right|_{\mathbf{p}=\mathbf{p}_k} \delta \mathbf{p}_{k+1} = -\mathbf{r}(\mathbf{p}_k) \quad . \tag{26}$$

The solution of the above linear system gives the correction term $\delta\mathbf{p}_{k+1}$, which is used to update $\mathbf{p}_k$ to obtain $\mathbf{p}_{k+1}$. If the scheme is convergent, the norm of the residual $\mathbf{r}(\mathbf{p}_k)$ should eventually vanish. Differentiating Eq.25 with respect to **p** and evaluating the resulting expression at the *k*th iteration gives

$$\frac{\partial \mathbf{r}(\mathbf{p})}{\partial \mathbf{p}} = (\boldsymbol{S}_k)^T (-\frac{\partial \boldsymbol{y}}{\partial \mathbf{p}})_k + \left(\frac{\partial (\boldsymbol{S}^T)}{\partial \mathbf{p}} \right)_k (\mathbf{e} - \mathbf{y}(\mathbf{p}_k)) \quad . \tag{27}$$

Recalling that $\mathbf{S} = \frac{\partial \mathbf{y}}{\partial \mathbf{p}}$ by definition, Eq.23 can be written as

Maejo Int. J. Sci. Technol. **2022**, *16*(03), 275-290

$$\frac{\partial \mathbf{r}(\mathbf{p})}{\partial \mathbf{p}} = (\mathbf{S}_k)^T \mathbf{S}_k + \left(\frac{\partial (\mathbf{S}^T)}{\partial \mathbf{p}} \right)_k (\mathbf{e} - \mathbf{y}(\mathbf{p})_k) = \mathbf{0} \quad . \tag{28}$$

The change in sensitivity matrix with respect to a change in **p**, i.e. $\frac{\partial \boldsymbol{S}}{\partial \mathbf{p}}$, is a second-order term and is usually ignored to decrease the computational complexity of the iterative scheme. Since the scheme described by Eq.26 is iterative, it will still converge to the correct value with this simplification as long as residual **r**(**p**) is exactly evaluated. With this consideration, the linearised system of Eq.26 can be written as

$$[(\boldsymbol{S}_k)^T \boldsymbol{S}_k](\delta \mathbf{p}_{k+1}) = (\boldsymbol{S}_k)^T (\mathbf{e} - \mathbf{y}(\mathbf{p})_k) \quad . \tag{29}$$

Once the system is solved, the current estimate for the ischemic region parameters $\mathbf{p}_k$ is updated as

$$\mathbf{p}_{k+1} = \mathbf{p}_k + \delta \mathbf{p}_{k+1} \tag{30}$$

and the procedure is repeated.

If the torso potentials are estimated at *n* points, then the sensitivity matrix $\mathbf{S} = \frac{\partial \boldsymbol{y}(\mathbf{p})}{\partial \mathbf{p}}$ for our problem will be

$$\mathbf{S} = \begin{bmatrix} \frac{\partial y_1}{\partial a} & \frac{\partial y_2}{\partial a} & \cdots & \frac{\partial y_{n-1}}{\partial a} & \frac{\partial y_n}{\partial a} \\ \frac{\partial y_1}{\partial b} & \frac{\partial y_2}{\partial b} & \cdots & \frac{\partial y_{n-1}}{\partial b} & \frac{\partial y_n}{\partial b} \\ \frac{\partial y_1}{\partial c} & \frac{\partial y_2}{\partial c} & \cdots & \frac{\partial y_{n-1}}{\partial c} & \frac{\partial y_n}{\partial c} \\ \frac{\partial y_1}{\partial d} & \frac{\partial y_2}{\partial d} & \cdots & \frac{\partial y_{n-1}}{\partial d} & \frac{\partial y_n}{\partial d} \end{bmatrix} , \tag{31}$$

where y_l indicates the FE outcome for torso potentials at the *l*th node. The derivative terms in the above matrix are evaluated numerically by changing each time one of the parameters (*a*, *b*, *c* or *d*) slightly, running the FE simulation with this set of parameters, observing the change in y_l values and calculating $\frac{\Delta y_l}{\Delta p_m}$ for the parameter p_m. Each FE run will produce one row of the ***S*** matrix.

Programming of Inverse Problem of ECG

The solution of the inverse problem involves running an FE forward analysis repeatedly with an updated **p** vector, hence an updated location of the ischemic region in the heart. Consequently, a general FE code is written to solve the forward problem in Python language. The forward FE code is embedded into a custom-made Python optimisation code, which calculates the sensitivity from the FE results of the current iteration and updates the parameter vector **p**, and reruns the forward FE code with the updated data for the next iteration. The optimisation scheme is schematically described in Figure 2.

Maejo Int. J. Sci. Technol. **2022**, *16*(03), 275-290

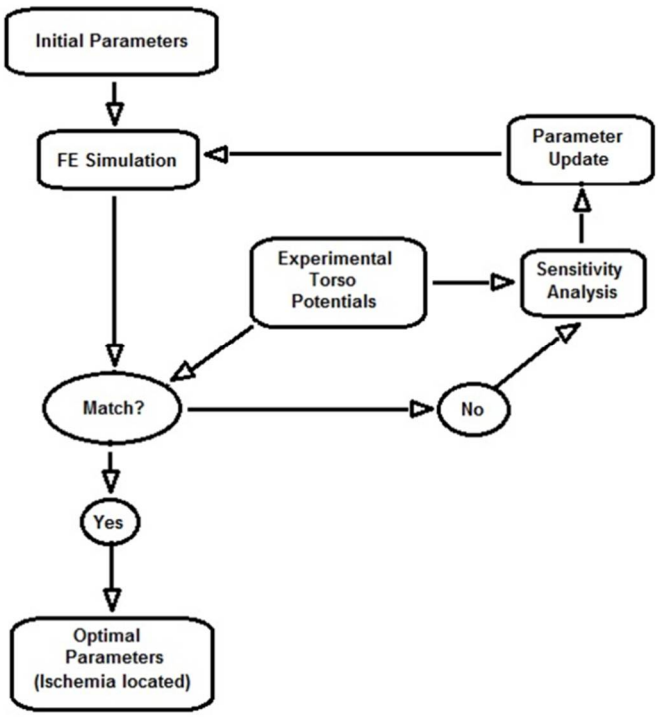

Figure2. Flowchart of optimisation algorithm

Example Problem

The methods of solving inverse problems are often tested with data created with the related forward analysis. In this work pseudo-experimental data for ischemic TMP reconstruction is produced by inducing ischemia to a certain location in the geometry and running the forward simulation. The resulting potentials at a specified set of nodes on the outer surface of the chest are taken as the experimental data. (These are equivalent to the actual ECG recordings taken at the chest.)

The geometric model for this study corresponds to a single two-dimensional slice located 50 mm above the apex of the heart (Figure 3). It is obtained from MRI data publicly available from University of Utah resources [41]**.** Realistic conductivities are taken from the literature and assigned to different tissues as well as to the healthy and ischemic heart tissues [42].

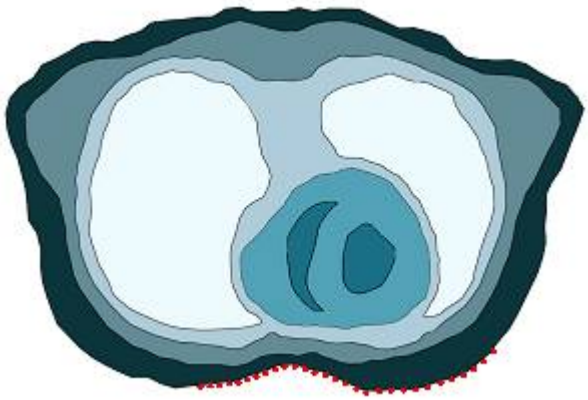

Figure 3. Nodes where virtual chest potentials are measured (red dots)

Maejo Int. J. Sci. Technol. **2022**, *16*(03), 275-290

The method is tested on three ischemia scenarios. In each one an ischemic region is placed at a different spot in the heart geometry, referred to as Ischemia 1, Ischemia 2 and Ischemia 3 in this text (Figures 4-6). As described above, the ischemic region is distinguished from the healthy tissue through its altered TMP. The forward analysis is run for all three cases to produce corresponding virtual ECG data measured at the outer torso surface (red dots in Figure. 3). Using these data, the sensitivity-based FE optimisation scheme is started with an initial estimate of ischemic region location that is far from its actual location. In a convergent scheme, as the parameters (a, b, c and d) evolve iteratively, the ischemic region should approach its actual location. It is observed whether the iterative process here is convergent in that sense.

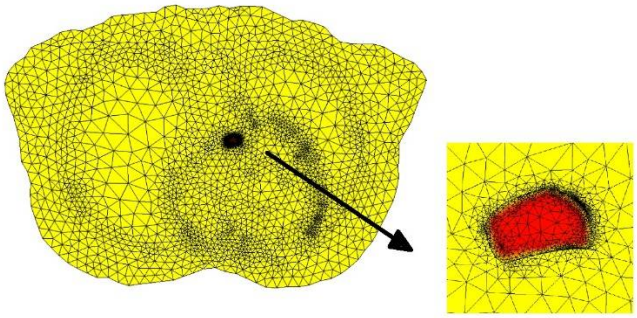

Figure 4. Torso model and ischemic region on posterior wall of heart (Ischemia 1) with applied TMP indicated

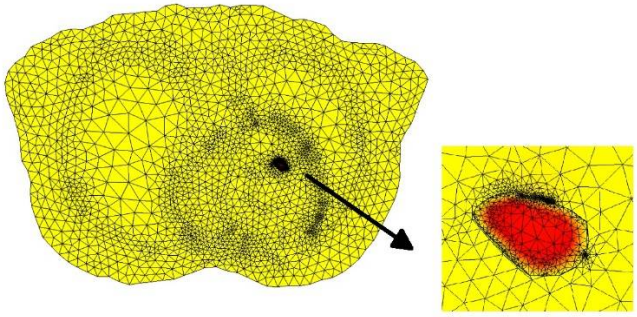

Figure 5. Torso model and ischemic region on left ventricle (Ischemia 2) with applied TMP indicated

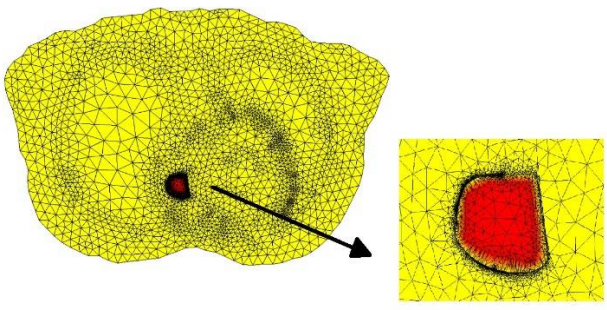

Figure 6. Torso model and ischemic region on right ventricle (Ischemia 3) with applied TMP indicated

Maejo Int. J. Sci. Technol. **2022**, *16*(03), 275-290

Since the main focus is to identify the location of the ischemic region, capturing the exact geometry of the ischemic region is not a concern in this method. Yet, the size of the assumed rectangular shape per Eq.1 will be a good indicator of the actual size of the ischemic region. If part of this region falls beyond the limits of the heart boundary during the optimisation iteration, the algorithm disregards that part. Hence it may be possible that the converged ischemic region is truncated. Furthermore, the patch of identified ischemic elements in the irregular FE mesh will look like a polygon rather than a rectangle.

RESULTS

Iteration 1 (Figures 7–9) refers to the initial estimate of the ischemic region and the proposed iterative scheme is able to converge to the correct ischemic area in all cases (shown in gray colour in the Figures). In Ischemia 1 (Figure 7) the ischemic region is located at the posterior wall of the heart. The approximate location of the ischemic region is captured in about the 15th iteration and the exact location is found in the 35th iteration. The convergence in this case of ischemia is observed to be slower than in the other two cases.

In Ischemia 2 (Figure 8) the ischemia is transmural: it covers the entire thickness of the left-ventricular wall. The approximate location of ischemia is identified in about the 12th iteration and the exact location is found in the 32nd iteration. In Ischemia 3 scenario (Figure 9) the ischemic region is closer to the anterior side of the heart located in the right ventricle and larger in size compared to the previous cases. As a result, the convergence is visibly faster in this case. After the 7th iteration, the estimated ischemic region is relatively close to the actual one, which is then captured in the 26th iteration.

In general, we have observed that an ischemic region closer to the observation sites (red dots in Figure 3) or larger in size causes a larger shift in the recorded potential (which corresponds to the ST segment shift in ECG). In those cases, the iterative scheme seems to converge faster. Also, in the first few iterations, the estimated ischemic region changes significantly from one iteration to the next. Typically, the approximate location of the ischemic region is established before the first half of the iterations is performed. The remaining iterations are dedicated to the fine-tuning of the boundaries of the ischemic region.

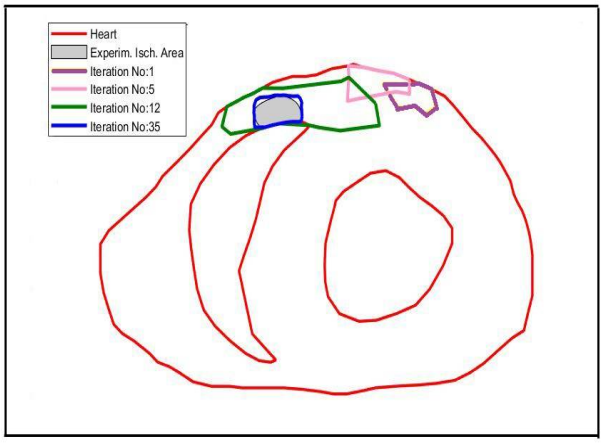

Figure 7. Localising anisotropic ischemic region using FE optimisation (Ischemia 1)

Maejo Int. J. Sci. Technol. **2022**, *16*(03), 275-290

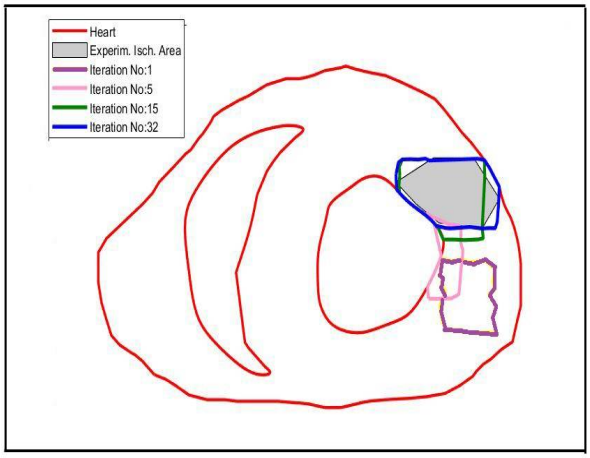

Figure 8. Localising anisotropic ischemic region using FE optimisation (Ischemia 2)

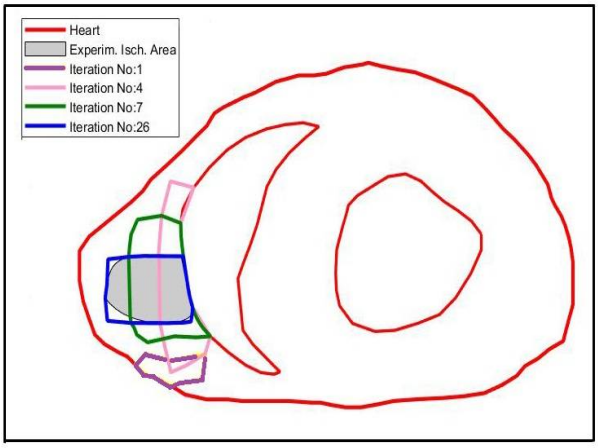

Figure 9. Localising anisotropic ischemic region using FE optimisation (Ischemia 3)

DISCUSSION AND CONCLUSIONS

In this work we have proposed a new numerical approach to tackling the inverse problem of ECG in order to locate the ischemic region in the heart from the ECG readings. The method relies on iterative FEM optimisation where the four parameters (a, b, c and d in Eq.16) describing the ischemic region location are iterated through sensitivity analysis.

Computational modelling of the electrical activity of the heart has been an active research area for more than three decades. During this period, the related literature has grown vast and the proposed models have increasingly become more detailed and sophisticated, evolving from two-dimensional to three-dimensional, from homogeneous to inhomogeneous, and from isotropic to anisotropic.

Sensitivity-based optimisation is a novel and promising technique for tackling the inverse problem of ECG that has been proposed in the present work. The functional form given by Eq.3 regularises the TMP and prevents it from taking an arbitrary distribution. On the other hand, with the conventional approach prescribed by Eq.2, an appropriate regularisation matrix **L** must be chosen to regularise the TMP distribution and a search for the optimal value of the parameter α must be performed. This requires the repeated solution of the linear system formed from Eq.2, sometimes using hundreds of different α values.

The only study that bears partial resemblance to this method in its iterative characteristics seems computationally more demanding than the one we have proposed. In this work Nielsen et al [43] performed an optimisation over the entire set of degrees of freedom on the heart geometry (i.e. nodal potentials of the FE mesh of the heart) in a two-dimensional problem subject to certain constraints, and convergence to the correct ischemic region occurred around the 40^{th} iteration. On the other hand, our scheme optimises only four parameters and requires less computation time.

The sensitivity-based iterative method has the potential for being an alternative to the existing regularisation-based techniques. We have illustrated the method on a two-dimensional problem but it can be easily extended to a three-dimensional one. In this case the TMP given in Eq.16 will take an extra term to account for the variation along the z-axis, which will introduce two additional parameters. The optimisation will be performed with respect to six parameters and the ischemic region will be a polyhedral mesh patch that resembles a rectangular prism.

In the mathematical modelling of ischemia, the pathology is usually modelled by imposing an altered TMP to the diseased tissue but assuming a healthy conductivity. The conductivity change that comes with this pathology has been only recently incorporated into some models, where epicardial potentials are estimated with the finite volume method in 3D models [44, 45]. In this work we have incorporated the conductivity change that comes with ischemia into our analysis. In a separate study (unpublished) we have assumed healthy conductivities when creating the pseudo-experimental data and when running the inverse analysis. The method has been equally effective in locating the ischemic region under these conditions.

REFERENCES

1. Y. Yamashita, "Theoretical studies on the inverse problem in electrocardiography and the uniqueness of the solution", *IEEE. Trans. Biomed. Eng.*, **1982**, *29*, 719-725.
2. D. Wang, R. M. Kirby, R. S. MacLeod and C. R. Johnson, "Inverse electrocardiographic source localization of ischemia: An optimization framework and finite element solution", *J. Comput. Phys.*, **2013**, *250*, 403-424.
3. C. E. Chávez, N. Zemzemi, Y. Coudière, F. Alonso-Atienza, and D. Álvarez, "Inverse problem of electrocardiography: Estimating the location of cardiac ischemia in a 3D realistic geometry", Proceedings of International Conference on Functional Imaging and Modeling of the Heart, **2015**, Maastricht, The Netherlands, pp.393-401.
4. Đ. Smiljana, R. Š. Marko, R. Miloš, A. Ć. Bojana and F. Nenad, "Finite Element Modelling of Cardiac Ischemia and Data Mining Application for Ischemic Detection and Localization", Proceedings of 18^{th} International Conference on Experimental Mechanics, **2018**, Brussels, Belgium, pp.1-6.
5. D. Wang, "Finite element solutions to inverse electrocardiography", *PhD Thesis*, **2012**, University of Utah, USA..
6. S. Stern, "State of the art in stress testing and ischaemia monitoring", *Card. Electrophysiol. Rev.*, **2002**, *6*, 204-208.
7. A. Pullan, "A high-order coupled finite element/boundary element torso model", *IEEE Trans. Biomed. Eng.*, **1996**, *43*, 292-298.
8. G. T. Lines, M. L. Buist, P. Grøttum, A. P. Pullan, J. Sundnes and A.Tveito, "Mathematical models and numerical methods for the forward problem in cardiac electrophysiology", *Comput. Vis. Sci.*, **2003**, *5*, 215-239.

9. A. Pullan, M. L. Buist and L. K. Cheng, "Mathematically modelling the electrical activity of the heart: from cell to body surface and back again", 1st Edn., World Scientific Publishing Co., Singapore, **2005**, pp.10-440.
10. A. N. Tikhonov and V. Y. Arsenin, "Solutions of Ill-posed Problems", V.H. Winston and Sons, Washington DC, **1977**, Ch. 2.
11. A. N. Tikhonov, A. V. Goncharsky, V. V. Stepanov and A. G. Yagola, "Numerical Methods for the Solution of Ill-Posed Problems", Kluwer Academic Publishers, Dordrecht, **1995**, Ch. 1.
12. J. P. Kaipio and E. Somersalo, "Statistical and Computational Inverse Problems", Springer, New York, **2005**, Ch.2.
13. V. Isakov, "Inverse Problems for Partial Differential Equations", Springer, New York, **2006**, Ch.2.
14. R. Huber, "Variational Regularization for Systems of Inverse Problems", Springer, Wiesbaden, **2019**, Ch.4.
15. A. Kirsch, "An Introduction to the Mathematical Theory of Inverse Problems". Springer, New York, **2021**, Ch.3.
16. B. J. Messinger-Rapport and Y. Rudy, "Regularization of the inverse problem in electrocardiography: A model study", *Math. Biosci.*, **1988**, *89*, 79-118.
17. Y. Rudy and B. J. Messigner-Rapport, "The inverse problem in electrocardiography: Solutions in terms of epicardial potentials", *Crit. Rev. Biomed. Eng.*, **1988**, *16*, 215-268.
18. C. R. Johnson and R. S. MacLeod, "Adaptive local regularization methods for the inverse ecg problem", *Prog. Biophys. Mol. Biol.*, **1998**, *69*, 405-423.
19. Y. Jiang, C. Qian, R. Hanna, D. Farina and O. Dossel, "Optimization of the electrode positions of multichannel ECG for the reconstruction of ischemic areas by solving the inverse electrocardiographic problem", *Int. J. Bioelectromagn.*, **2009**, *11*, 27-37.
20. B. Messnarz, B. Tilg, R. Modre, G. Fischer and F. Hanser, "A new spatiotemporal regularization approach for reconstruction of cardiac transmembrane potential patterns", *IEEE Trans. Biomed. Eng.*, **2004**, *51*, 273-281.
21. B. Yao, R. Zhu and H. Yang, "Inverse ECG modeling with spatiotemporal regularization for the characterization of myocardial infarctions", Proceedings of IEEE EMBS International Conference on Biomedical and Health Informatics, **2018**, Las Vegas, USA, pp.120-123.
22. Y. Wang and Y. Rudy, "Application of the method of fundamental solutions to potential-based inverse electrocardiography", *Ann. Biomed. Eng.*, **2006**, *34*, 1272-1288.
23. M. Tyšler, J. Lenková and J. Švehlíková, "Impact of the patient torso model on the solution of the inverse problem of electrocardiography", *Biomed. Eng.*, **2014**, *12*, 58-65.
24. M. Milanič, V.Jazbinšek, R. S. MacLeod, D. H. Brooks and R. Hren, "Assessment of regularization techniques for electrocardiographic imaging", *J. Electrocardiol.*, **2014**, *47*, 20-28.
25. F. M. Melgarejo-Meseguer, E. Everss-Villalba, M. Gutiérrez-Fernández-Calvillo, S. Muñoz-Romero, F. J. Gimeno-Blanes, A. García-Alberola and J. L. Rojo-Álvarez, "Generalization and regularization for inverse cardiac estimators", *IEEE Trans. Biomed. Eng.*, **2022**, *69*, 3029-3038.
26. K. W. Chen, L. Bear and C. W. Lin, "Solving inverse electrocardiographic mapping using machine learning and deep learning frameworks", *Sensors*, **2022**, *22*, Art.no.2331.
27. J. Xie and B. Yao, "Physics-constrained deep learning for robust inverse ECG modeling", *IEEE Trans. Autom. Sci. Eng.*, **2022**, doi: 10.1109/tase.2022.3144347.

28. A. Cimponeriu, C. F. Starmer and A. Bezerianos, "A theoretical analysis of acute ischemia and infarction using ECG reconstruction on a 2-D model of myocardium", *IEEE Trans. Biomed. Eng.*, **2001**, *48*, 41-54.
29. R. M. Shaw and Y. Rudy, "Electrophysiologic effects of acute myocardial ischemia: A theoretical study of altered cell excitability and action potential duration", *Cardiovasc. Res.*, **1997**, *35*, 256-272.
30. B. F. Nielsen, M. Lysaker and P. Grottum. "Computing ischemic regions in the heart with the bidomain model– First steps towards validation", *IEEE Trans. Med. Imaging*, **2013**, *32*, 1085-1096.
31. M. C. MacLachlan, B. F. Nielsen, M. Lysaker and A. Tveito, "Computing the size and location of myocardial ischemia using measurements of ST-segment shift", *IEEE Trans. Biomed. Eng.*, **2006**, *53*, 1024-1031.
32. E. Carmeliet, "Cardiac ionic currents and acute ischemia: From channels to arrhythmias", *Physiol. Rev.*, **1999**, *79*, 917-1017.
33. R. S. MacLeod, S. Shome, J. Stinstra, B. B. Punske and B. Hopenfeld, "Mechanisms of ischemia-induced ST-segment changes", *J. Electrocardiol.*, **2005**, *38*, 8-13.
34. P. R. Johnston, "The effect of simplifying assumptions in the bidomain model of cardiac tissue: Application to ST segment shifts during partial ischaemia", *Math. Biosci.*, **2005**, *198*, 97-118.
35. B. F. Nielsen, X. Cai and M. Lysaker, "On the possibility for computing the transmembrane potential in the heart with a one shot method: An inverse problem", *Math. Biosci.,* **2007**, *210*, 523-553.
36. M. C. MacLachlan, J. Sundnes, O. Skavhaug, M. Lysaker, B. F. Nielsen and A.Tveito, "A linear system of partial differential equations modeling the resting potential of a heart with regional ischemia", *Math. Biosci.*, **2007**, *210*, 238-252.
37. M. C. MacLachlan, J. Sundnes and G. T. Lines, "Simulation of ST segment changes during subendocardial ischemia using a realistic 3-D cardiac geometry", *IEEE Trans. Biomed. Eng.*, **2005**, *52*, 799-807.
38. T. S. Ruud, B. F. Nielsen, M. Lysaker and J. Sundnes, "A computationally efficient method for determining the size and location of myocardial ischemia", *IEEE Trans. Biomed. Eng.*, **2009**, *56*, 263-272.
39. M. K. Ün and A. Çalık, "Estimation of depth-dependent material properties of biphasic soft tissues through finite element optimization and sensitivity analysis", *Med. Eng. Phys.*, **2019**, *74*, 73-81.
40. V. Arbabi, B. Pouran, G. Campoli, H. Weinans and A. A. Zadpoor, "Determination of the mechanical and physical properties of cartilage by coupling poroelastic-based finite element models of indentation with artificial neural networks", *J. Biomech.*, **2016**, *49*, 631-637.
41. The Scientific Computing and Imaging Institute, "Datasets", **2007**, https://sci.utah.edu/sci-software/datasets.html (Accessed: February 2017).
42. S. E. Geneser, R. M. Kirby and R. S. MacLeod, "Application of stochastic finite element methods to study the sensitivity of ECG forward modeling to organ conductivity", *IEEE Trans. Biomed. Eng.*, **2008**, *55*, 31-40.
43. B. F. Nielsen, M. Lysaker and A.Tveito, "On the use of the resting potential and level set methods for identifying ischemic heart disease: An inverse problem", *J. Comput. Phys.*, **2007**, *220*, 772-790.

Maejo Int. J. Sci. Technol. **2022**, *16*(03), 275-290

44. B. M. Johnston and P. R. Johnston, "Sensitivity analysis of ST-segment epicardial potentials arising from changes in ischaemic region conductivities in early and late stage ischaemia", *Comput. Biol. Med.*, **2018**, *102*, 288-299.
45. B. M. Burton, K. K. Aras, W. W. Good, J. D. Tate, B. Zenger and R. S. MacLeod, "Image-based modeling of acute myocardial ischemia using experimentally derived ischemic zone source representations", *J. Electrocardiol.*, **2018**, *51*, 725-733.